Journal of the American Helicopter Society

April [illegible] Volume [illegible] Number [illegible]

AMERICAN HELICOPTER SOCIETY

Results from the NASA Automated Nap-of-the-Earth Program





Richard E. Zelenka Phillip N. Smith Richard A. Coppenbarger Chima E. Njaka Banavar Sridhar
NASA Ames Research Center, Moffett Field, CA

Military helicopter Nap-of-the-Earth (NOE) flight is one of the most demanding low-altitude, near terrain flight operations. In NOE, the pilot is operating at or below tree-top levels, taking maximum advantage of the terrain and ground features for concealment. Such increased proximity to obstructions places heightened maneuverability requirements on the aircraft and extreme levels of workload on the pilot.

The basic issue being addressed in the NASA Automated Nap-of-the-Earth (ANOE) program is the intelligent use of environmental information such as knowledge of terrain, obstacles, and other external factors to enhance the flight path guidance of the vehicle. This is a major departure over contemporary guidance and control based on feedback of state variables such as vehicle attitudes, velocities, and accelerations. Although the immediate program has a military focus, the technological advances inherent for automating NOE flight have great benefit to the operation of a wide class of vehicles such as emergency medical helicopters, conventional and high-speed transports, unmanned aerial vehicles, and planetary vehicles.

This paper summarizes results to date of the NASA ANOE program in the areas of passive and active sensors, pilot displays, low-altitude manual trajectory guidance, and NOE automatic guidance. Each of these areas has been developed and evaluated in piloted, motion-based simulation or through flight test. These evaluations have demonstrated the feasibility of automating the NOE flight mission, and have generated additional spin-off applications of the technologies.

Introduction

Pilots flying rotorcraft close to the ground in nap-of-the-earth flight are confronted with unique guidance and control tasks such as aircraft concealment, obstacle avoidance, and long-range mission planning. These flight tasks require a high degree of skill and concentration, and can be intensified by low-visibility and high auxiliary workload conditions. Automation in this flight regime is desired to reduce pilot workload without compromising pilot confidence and safety.

The objective of the NASA Automated Nap-of-the-Earth program is to aid the helicopter pilot during low-altitude and NOE flight through computer and sensor augmentation. The program has focused on three technology areas: (1) processing methods for acquiring terrain and obstacle information from passive and active sensors, (2) use of stored digital terrain data in conjunction with highly accurate navigation systems for improved low-altitude guidance, and (3) augmentation of stored digital terrain data through the use of forward-looking sensors and integration of these sensor data into the flight guidance and control systems for manual and automatic modes.

All three technology areas involve conceptualization, analysis, hardware implementation, and flight test. The first and third technology areas were flight tested on the NASA/Army UH-60 RASCAL (Rotorcraft Aircrew Systems Concepts Airborne Laboratory) test helicopter. The second technology area was accomplished in joint flight test with the U.S. Army on the Army UH-60 STAR (Systems Testbed for Avionics Research) test helicopter. The NASA VMS (Vertical Motion Simulator) facility has been used extensively, in conducting piloted, motion-based high fidelity graphic flight simulations. Because automating nap-of-the-earth flight is such a revolutionary concept, the piloted evaluation studies include concepts for low-altitude (above tree-top) as well as NOE (below tree-top) flight. These conceptual aids have direct application to certain missions (e.g. military special operations, search and rescue) and offer the potential of being a first step in piloted automation in proximity to terrain.

The NASA ANOE program includes the following component technologies:

1. *Passive Sensors:* use of "pixel-flow" data from television and infrared cameras to detect and extract range and position to objects and terrain. Such sensors offer high update rates and wide field of views without emitting energy.
2. *Active Sensors:* use of millimeter wave (MMW) radar and laser radar to detect and measure range and position to objects and terrain. These sensors offer accurate ranging to objects, fine resolution, and operation in degraded weather conditions.
3. *Mid-field, Low-Altitude Manual Guidance System:* use of navigational, aircraft state, terrain database, forward sensor information, and pilot displays to present an above-the-treetops trajectory to the pilot using manual control.
4. *Near-field, Pilot-Directed Automated Guidance System:* use of aircraft state information, terrain database, forward sensors, and pilot displays to provide a below tree-top NOE trajectory to the pilot, providing automatic control maneuvers in the event of a potential ground or obstacle collision.

This paper describes the results of the NASA ANOE program in the above technical component areas, summarizes the programs findings, and provides future program directions.

Presented at the American Helicopter Society 52nd Annual Forum, Washington, D.C., June 4-6, 1996. Manuscript submitted April 1996; accepted Nov. 1996.

Overall ANOE System Architecture

The complete automated NOE system uses a terrain / obstacle database in generating trajectory guidance, which is presented to the pilot through a helmet-mounted display. Maneuvering the aircraft along the recommended trajectory is directed by the pilot, although assisted through automatic control. At his discretion, the pilot may elect to delegate complete maneuvering control of the aircraft to the automatic system. It is unlikely, however, that fully automatic operation will be typical, as pilots are justifiably unwilling to relinquish total authority to any automatic system. Our automated NOE system architecture is shown as Fig. 1.

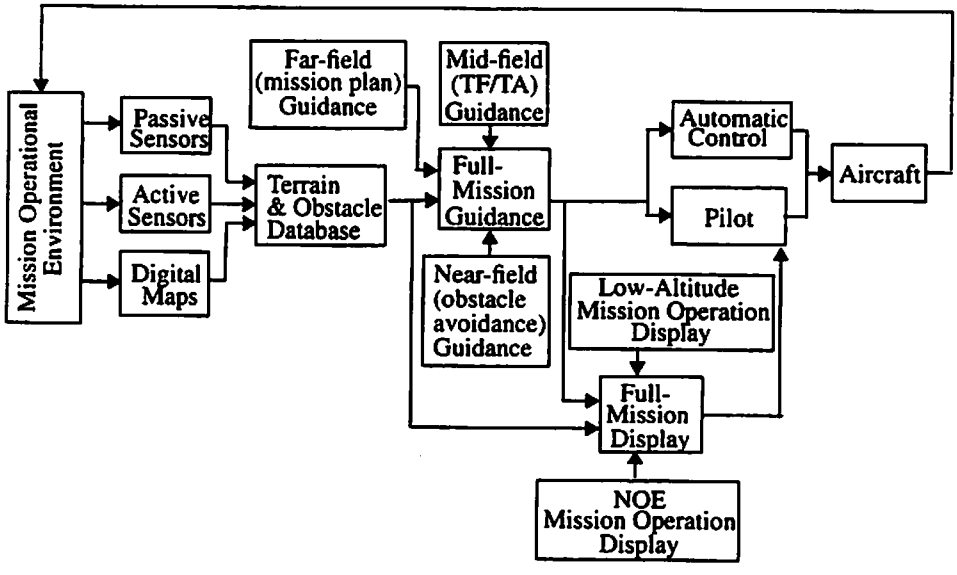

Fig.1. Overall Automated NOE system architecture.

A combination of forward sensors and digitized terrain elevation maps provides the required far, mid, and near-field planning (Refs. 1, 2). "Far-field" or mission planning yields coarse waypoints several miles apart and takes into account mission requirements and global threat information. Existing mission or route planners, drawing from relatively coarse digitized terrain maps, are sufficient for this purpose (Refs. 3, 4). High resolution digital maps commonly available from the U.S. Defense Mapping Agency (~100m resolution) (Ref. 5) are required to provide mid-field trajectory planning. These maps allow a low-altitude, short duration (~1 minute), "mid-field" valley-seeking guidance trajectory to be generated and to refine the far-field route (Ref. 6). Valley-seeking, lateral and vertical maneuvering flight is commonly termed terrain following / terrain avoidance (TF/TA) flight.

Non-energy-emitting passive sensors, such as video cameras or forward-looking infrared (FLIR), and those that actively emit energy, e.g. radar and laser radar, are necessary for "near-field" planning. Near-field planning adjusts the mid-field guidance trajectory with regard to unmapped obstacles, such as trees, wires, and structures. Most digitized terrain maps do not include these obstacles, and those that do cannot account for hazards placed after map sampling, a likely event even in non-hostile environments. These passive and active forward sensors update the digitized terrain maps with high resolution, high accuracy terrain and obstacle information which can then be used for close-in, near-field obstacle avoidance.

Passive sensors, which use the parallax between image frames to obtain ranging to obstacles, have the advantages of high update rates, wide field of views, and covertness. However, they are limited in degraded weather and typically produce sparsely populated, non-uniform obstacle maps. Their resolution is not fine enough for wire detection. Active sensors, such as millimeter-wave (MMW) radar or laser radar (ladar), provide much denser, more uniform obstacle maps. MMW radar operates in degraded weather, while ladar (and some radar bands) can detect wires. Active sensors typically provide low update rates for fields of view comparable to passive sensors. As such, both types of these complementary sensors are required for near-field obstacle detection and avoidance.

Full-mission guidance is the result of combining far-field mission planning guidance, mid-field low-altitude TF/TA guidance, and near-field obstacle avoidance guidance. This combined guidance function is then presented to the pilot on a pilot-centered full-mission display. This display includes modes for low-altitude TF/TA operations and for NOE operations. These displays are intimately coupled with the degree of control allotted to the automatic system. The level of automation and associated pilot interface strongly influence pilot acceptability, which is crucial to the realistic success of an automated NOE system.

ANOE Program Component Technologies

Passive Sensors

Electro-optical sensors, such as visible- and infrared-band cameras, offer wide field-of-view and a fast update rate for obstacle detection and ranging applications without radiating energy. Earlier systems using these sensors relied on extensive a priori knowledge of the objects to be detected and/or interaction with a human user to designate objects of interest. In the NOE application where the role of the sensors is to detect unexpected objects (i.e., those not appearing in digital terrain maps) and to aid in reducing the pilot's workload, neither of these assumptions apply. In addition, the sensor must determine the position of detected obstacles.

Approach

Beginning in 1986, the theoretical foundation for the obstacle detection and ranging algorithms was established (Ref. 7). Given the ability to measure the motion of an object between frames in an image sequence and measurements of the camera's motion state, a Kalman filter was developed to estimate the object's position (range, azimuth, and elevation) under the assumption that the object is not moving. This approach allows for detection and ranging under the full 6 degree-of-freedom maneuvering expected during NOE operations.

Implementation and Flight Test Results

Following initial laboratory demonstrations and testing (Refs. 8-10), flight test data were collected to support development and validation of the single-camera obstacle detection and passive range estimation algorithms. A single monochrome camera was mounted in the nose of a CH-47 Chinook helicopter. Aircraft state information was measured using an inertial navigation system (INS). Truth measurements of obstacle positions relative to the helicopter were obtained using a ground-based laser tracking system. Off-line results using these flight data demonstrated the ability to detect objects at a distance of up to 700 feet and to estimate range within 10 percent error by the time the helicopter had travelled one-tenth the dis-

tance toward the object (Ref. 11).

The initial approach was expanded to incorporate multiple cameras to overcome limitations in ranging to objects directly along the helicopter's path (Ref. 12). In addition, enhancements to the range-estimation filter resulted in an improved capability for ranging to distant objects (Ref. 13). Development of the multi-camera ranging algorithms led to a follow-on flight test in which two cameras were mounted one meter apart on the nose of a UH-60 Blackhawk helicopter. Fig. 2 shows the NASA/Army RASCAL test helicopter (Ref. 14) equipped with stereo outboard visible-band cameras and an infrared centerline camera. A Litton LN-93 INS and an Ashtech differential GPS system provided the aircraft state information. As before, a ground-based laser tracker was used to measure the true obstacle positions for validation of the passive ranging algorithms. Analysis of the resulting data showed improved range accuracy and an extended range to 1000 feet (Ref. 15). A summary of passive ranging results obtained from flight test is provided in Fig. 3 and Table 1. The flight test scenario included several trucks parked on a runway that were detected during a 3 deg glide-slope landing.

Having validated through flight data the feasibility of obstacle detection using passive sensors, our focus shifted to achieving real-time operation. An estimated 2 billion floating point operations per second were required to achieve real-time performance of the multi-camera algorithm at a rate of 15 frame-pairs per second. Since this computational requirement was beyond the capability of off-the-shelf microprocessors and digital signal processors, parallel processing technology was employed. The selection of a parallel processing architecture addressed trade-offs in overall speed increase, processor utilization, programmability, and physical constraints. In addition, the processing system needed to accommodate changes in the vision algorithm, exhibit good scalability, and be able to be installed on a helicopter. Multi-processor architectures investigated included a traditional image processing architecture, a shared-memory system, and two distributed-memory machines (Ref. 16-20). The most promising architecture, a distributed-memory multi-processor machine, was successfully implemented under a Small Business Innovative Research (SBIR) contract awarded to Innovative Configurations, Inc. The resulting system uses 32 Intel i860 processors and a stereo image acquisition system implemented on three 9U VME computer boards to detect and range to 300 "objects" at an update rate of 15 Hz. An object is an entity trackable through passive ranging algorithms, such as a physical object's edge or corner. The truck obstacles of Fig. 3 commonly provided several dozen objects for tracking.

Fig. 2. Test helicopter with stereo cameras (outboard) and infrared camera (center) during data collection flights.

Fig. 3. Truck obstacles parked on runway during final approach landing sequence.

Table 1. Summary of passive ranging results given imaging sequence of Fig. 3.

Truck	Frame	Truth Range (ft)	Monocular Range (ft)	Motion/Stereo Range (ft)
A	1	488	171	489
	60	399	405	431
	120	316	335	350
	180	235	227	247
B	1	614	270	785
	60	525	568	587
	120	443	462	463
	180	363	364	341
C	1	741	267	739
	60	650	519	498
	120	568	606	565
	180	487	514	486
D	1	860	138	n/a
	60	770	618	594
	120	688	653	799
	180	609	534	671
E	1	991	122	955
	60	899	995	813
	120	817	594	698
	180	736	863	722

Following laboratory testing, the real-time passive ranging system was modified for airborne operation and installed on the NASA/Army UH-60 RASCAL helicopter for flight demonstration. The system obtained all required inputs directly from aircraft sensors in demonstrating real-time passive ranging capability at low altitude under full 6 degree-of-freedom maneuvering.

Active Sensors

Active sensors are capable of operating in degraded weather with precise ranging measurements, but at slower update rates for comparable field of views to passive sensors. The millimeter-wave (MMW) band provides small antennas with narrow beam shapes, which, when configured as a "pencil-beam" 3-d radar, provides precise range, azimuth, and elevation to obstacles and terrain. This allows great flexibility in implementation and use of the radar information beyond that required for the near-field guidance planning of ANOE flight.

Approach

The scanning, pencil-beam MMW radar allows a terrain and obstacle database (TOD) to be constructed and presented to the pilot as a synthetic perspective display. This display would be of greatest benefit during flight operations in unfamiliar areas, such as those encountered during heliborne emergency medical service (EMS), search and rescue, and airborne fire-fighting missions.

Implementation

NASA collaborated with Honeywell in developing a 35 GHz pulsed radar system for use in the NASA ANOE program and for use as a stand-alone collision protection and warning device. The NASA/Honeywell 35 GHz coherent pulsed MMW radar system takes advantage of existing 4.3 GHz radar altimeter components in performing the transmit and receive functions. The 4.3 GHz signal is passed through an upconverter to 35 GHz, and emitted as a scanning, pencil-beam through a twist-reflector type antenna. Radar returns are down-converted to 4.3 GHz and processed using the 4.3 GHz radar altimeter components. 35 GHz affords good weather penetration capability and scattering at low grazing angles, and a small antenna (11.8 in diameter).

The resulting 2.6 deg pencil-beam is scanned over a 20 deg elevation by 50 deg azimuth field of view in 1 sec (fully interlaced in 2 sec). Range gating varies from 16 to 32 ft over the 1056 ft range of the radar. The radar system was designed to allow growth in range to 10,000 ft. An early single-beam, non-scanning version of this radar demonstrated excellent correlation between predicted and flight test performance (Ref. 21).

The radar-derived TOD is presented to the pilot on a panel-mounted display as a 3-dimensional synthetic perspective "grid" display. Each grid is drawn at the height estimated from current and prior radar returns, and any stored map data that may be available. The grid perspective display can also be overlaid onto a video image provided by a camera mounted adjacent to the radar.

An obstacle-sensitive guidance trajectory can be generated using the radar-derived terrain and obstacle database. Such a trajectory and associated display has been extensively flight tested through a NASA/Army low-altitude flight guidance program (Ref. 22). This work is described in the section on mid-field, low-altitude manual guidance.

Flight Test Results

Flights were conducted with the NASA/Honeywell 35 GHz radar on the NASA/Army UH-60 RASCAL test helicopter based at Ames Research Center. The 35 GHz radar was mounted on the nose of the aircraft on an experimental mounting bar, adjacent to a color video camera (Fig. 4). The camera allowed recordings of the perspective grid display with the camera video.

Flights were conducted during day VFR conditions in flat and moderately rugged mountainous terrain. Test profiles included flights among tower and wire obstacles. Speeds flown were between 20 - 60 kts, at altitudes of 200 ft AGL and below. Tests of the radar system found the radar capable of detecting low grazing angle terrain, towers and trees without difficulty. While the radar was not designed to detect wires and cables, it detected high tension transmission towers, and there were indications that it could intermittently detect the cables. It was assumed this occurred on multi-stranded cables where the reflection from the wires was diffuse rather than the more specular reflection produced from smooth wires.

The 3-dimensional grid-world perspective view display was able to be reliably constructed and rendered in real-time from the radar's returns, creating a fairly accurate representation of the scene surrounding the helicopter. However, the current limited range did require flights at low-altitude and speed so as to not "over-fly" the field of view and range of the sensor (Ref. 23). Fig. 5 depicts a representative radar-generated grid display from flight test, in which the aircraft was heading toward a hill with an adjacent (left) tower. The radar and associated display demonstrated the system's potential usefulness for collision avoidance. Further results are found in Ref. 23.

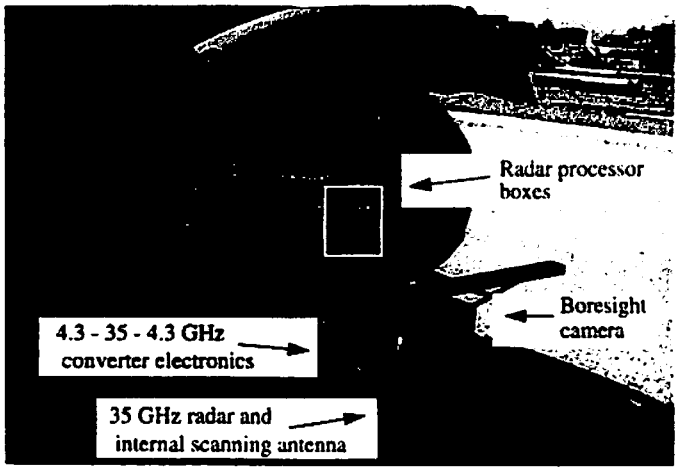

Fig. 4. Test helicopter with NASA/Honeywell 35 GHz MMW radar.

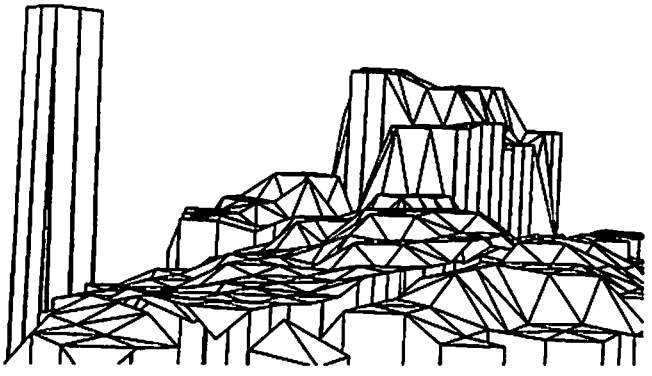

Fig. 5. Perspective grid-world display in hilly terrain with adjacent tower obstacle.

Mid-Field, Low-Altitude Manual Guidance System

A mid-field low-altitude terrain following / terrain avoidance (TF/TA) guidance system relying on digitized terrain elevation maps was developed that employs airborne navigation, mission requirements, aircraft performance limits, and radar altimeter returns to generate a valley-seeking, low-altitude trajectory between waypoints in real-time. "Mid-field" refers to planning of approximately 1 minute ahead and low-altitude is taken as no lower than tree-top altitude. By applying a cost function over an intended route between waypoints, a three-dimensional TF/TA route may be calculated in real-time.

Approach

The trajectory generation algorithm maintains a cost function that seeks to minimize mean sea level (MSL) altitude, heading change from a straight line nominal path between waypoints, and lateral offset from the nominal path. The cost function is applied to candidate trajectories from the current aircraft position over discrete pitch and roll angles. The lowest cost function trajectory (for the next 30 sec) is then selected (Ref. 4). Ad

justing constants of the cost function allows varying degrees of weighting to be applied to each performance parameter. The pilot selects aircraft performance limits and constants for the system. These include maximum bank, climb and dive angles, normal load factor, and desired velocity and set clearance altitude. Set clearance altitude is that AGL altitude the guidance algorithm will seek. By severely penalizing, for example, those trajectories that deviate from the straight line nominal course (in heading and position), a straight line contour trajectory is generated. Such flight exclusively in the vertical plane is termed terrain following (TF) flight. Decreasing the penalty on these same two parameters allows lateral movement, and yields a meandering terrain following / terrain avoidance (TF/TA) flight profile. A general far-field flight plan, consisting of a series of course waypoints, is supplied by a mission planner or simply input by the crew, and can be changed in flight. The mission planner, if supplied with ground based threat information, will choose course waypoints sensitive to these hazards.

Implementation

The trajectory generated by the guidance system is presented symbolically to the pilot through a helmet mounted display (HMD), the Integrated Helmet and Display Sighting System (IHADSS). The Honeywell IHADSS is standard equipment for the U.S. Army's AH-64 Apache helicopter. A simplified pictorial of the "pathway-in-the-sky" pilot presentation symbology on the head-tracked HMD is shown as Fig. 6, which presents a climbing left turn trajectory.

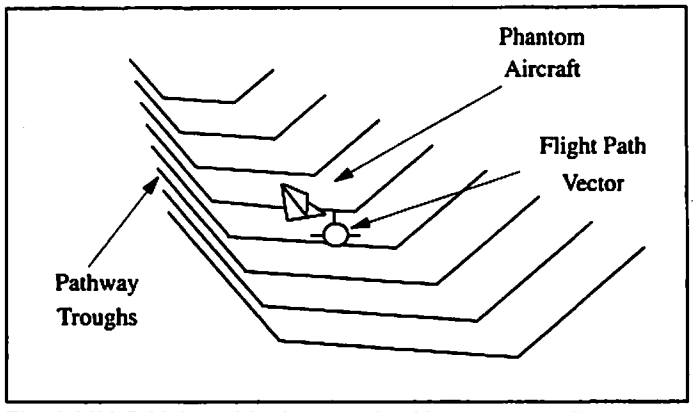

Fig. 6. Mid-field, low-altitude manual guidance system pilot symbology.

The pathway troughs and phantom aircraft are drawn in inertial space along the desired trajectory. The troughs are 100 ft (30.5 m) wide at the base, 50 ft (15.2 m) tall, and 200 ft (61.0 m) wide at top, and are drawn in 1 sec increments of the trajectory out to 8 sec, based on the aircraft's airspeed. The top center of each pathway is the desired, computed trajectory. The phantom aircraft flies at the top center of the fourth trough (the desired trajectory 4 s in the future). The aircraft's flight path vector is also drawn on the helmet mounted display, as predicted 4 s ahead. Hence, by tracking the phantom aircraft with the flight path vector, the pilot flies the desired TF/TA guidance trajectory. Additional aircraft state information also displayed (but not shown on Fig. 6) includes magnetic heading, engine torque, airspeed, altitude, and turn and slip. A horizon line, pitch ladder, and aircraft nose chevrons are also displayed to improve situational awareness. An airspeed flight director tape shows deviation from the pilot selected airspeed. This symbology set was developed over several piloted, motion-based simulations with a diverse group of pilots, and gives good trajectory tracking performance with low pilot workload. Such a "pilot-centered" display, providing trajectory lead information and heightened situational awareness, is preferred by pilots to traditional "flight-director" ILS-type displays (Ref. 24).

Piloted Simulation and Flight Test Results

The TF/TA guidance system evolved through four motion-based, piloted simulations on the NASA Ames Vertical Motion Simulator (VMS) facility. These simulations were used to develop the guidance algorithm, pilot display laws, and pilot display symbology, and included studies of individual display elements, pilot handling qualities ratings, and pilot workload. The TF/TA guidance system was evaluated during flight trials with the U.S. Army Command/Control Systems Integration Directorate (C2SID), Ft. Monmouth, NJ, on their NUH-60 STAR (Systems Testbed for Avionics Research) helicopter.

The guidance system was further validated through flight test and supporting VMS simulations in three phases; (1) the baseline terrain map-based system, (2) the radar altimeter Kalman filter system, and (3) the forward sensor equipped system, which added an obstacle avoidance capability. The phases built upon one another and progressively increased in complexity and capability (Fig. 7). The guidance system has been extensively flight tested in primarily rugged terrain in So. Central Pennsylvania. The baseline system's performance is principally limited in its ability to accurately position itself above the terrain, and its inability to detect and avoid unmapped obstacles, such as trees and wires. The above ground positioning limitation was dominant and restricted flight of the baseline system to above 300 ft AGL at the operational design speeds between 80 and 110 kts (Ref. 25).

The light, solid blocks of Fig. 7 detail the extension to the baseline TF/TA guidance system resulting from a Kalman filter augmentation. The predicted AGL altitude, calculated as the difference in the navigation system MSL altitude and the stored map terrain elevation, together with the radar altimeter measurement, are blended in a Kalman filter to yield an estimate for the difference error from the predicted AGL altitude. This difference error value, , is then used to alter the terrain elevation database referenced guidance trajectory at the AGL-error blending block. This modified trajectory is then presented to the pilot using the existing display laws and symbology. The enhancement produced trajectories more reflective of the topography and allowed for lower altitude operation than that of the baseline guidance system. The minimum flight altitude of this Kalman filter augmented system was reduced from 300 ft AGL altitude to 150 ft at operational speeds from 80 to 110 kts (Ref. 26). Flight restrictions for the terrain-referenced guidance system were now governed by pilot obstacle detection and avoidance, which could be assisted by a forward-looking sensor.

The third and final phase of the guidance system decreased the systems operational altitude to 75 ft AGL altitude and added an obstacle avoidance capability. The forward sensor enhancement to the NASA/Army mid-field manual guidance system involved the addition of three distinct components; a wide field of view forward looking laser radar, a terrain/obstacle database generated from sensor returns, and a path manager, which modifies the guidance trajectory if necessary after querying the sensor database. This enhancement is shown as bold blocks in Fig. 7.

The forward sensor was the Northrop Obstacle Avoidance System (OASYS) laser radar prototype sensor developed by the U.S. Army (Refs. 27, 28). The terrain and obstacles located by the forward sensor are stored in an inertially-referenced square grid periodically shifted so its center position remains below the aircraft. The database is updated with a group of OASYS detected objects at 10 Hz. A "path manager" is used to alter the guidance trajectory in the event of an altitude clearance problem, as determined by the elevations of obstacles and terrain stored in the sensor generated database. All adjustments made to the trajectory are in vertical position only, i.e. no lateral modifications are made.

A representative flight test result from a terrain following (TF) mission is shown as Fig. 8. Terrain following flight, or contour flight, is flown at constant heading between waypoints with only vertical maneuvering al-

lowed. The ground tracks are straight lines between waypoints. This TF mission was flown at 80 kts airspeed and set clearance altitude of 75 ft, creating expected guidance trajectory AGL clearances of 75 ft AGL and above. These figures trace the elevation or vertical track (Fig. 8a), as well as the pilot's tracking of the guidance trajectory through the HMD symbology previously discussed. The upper solid line traces the aircraft MSL altitude while flying the forward-sensor equipped guidance system. The upper dashed line tracks the desired (or "commanded") trajectory MSL altitude, which is computed by the trajectory algorithm as modified by the forward sensor dependent path manager and presented to the pilot. The difference between these two lines, representing the pilot's vertical tracking of the desired trajectory, is provided in Fig. 8b. The lowest solid line of Fig. 8a is the "truth" measurement of the terrain elevation, which is calculated as the aircraft's MSL altitude minus the radar altimeter measurement.

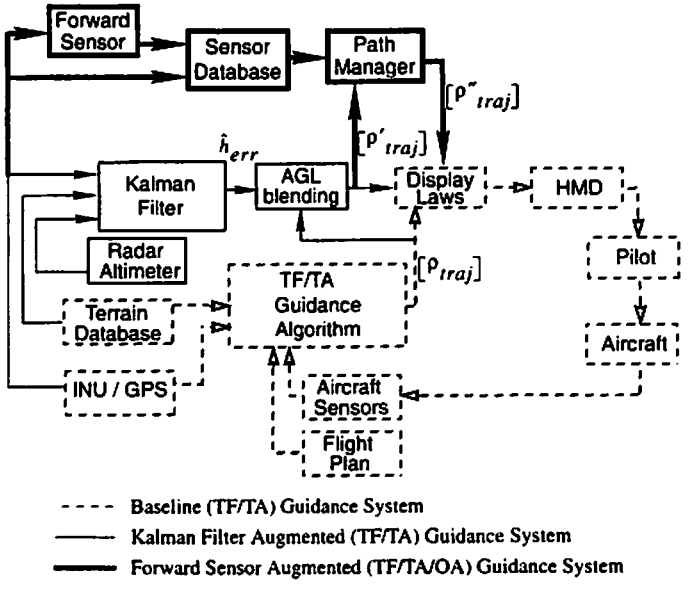

Fig. 7. Mid-field, low-altitude manual guidance system block diagram.

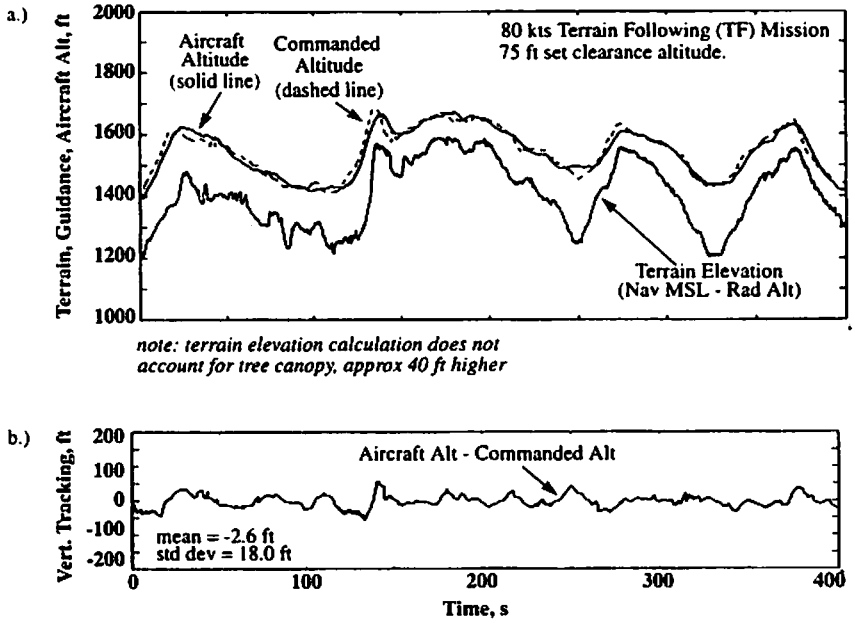

Fig. 8. Flight test results of low-altitude, manual guidance system. (a.) Elevation (vertical) profile. (b.) Pilot elevation tracking of guidance trajectory.

The commanded (path manager corrected) pathway of Fig.8a presents a smooth but aggressive trajectory. Terrain undulations are clearly recognized and reflected in the pathway placement. Areas where the guidance pathway appears too high are most likely due to local foliage effects, i.e. a tight, higher concentration of trees, or the effect of the smooth flight path angle constraint imposed on all guidance trajectories. Fig. 8b shows the difference between the elevation (vertical) command position and that of the aircraft. Mean elevation tracking was -2.6 ft, with standard deviation of 18.0 ft. Except for the period surrounding the hill just prior to time 150 s, tracking is within the trough vertical bounds of 50 ft. Imperfect trajectory tracking can be traced to two principle reasons; the pilot can never track the symbology perfectly, and at times will override the recommended pathway. Circumvention of the commanded trajectory occasionally occurs when a pilot "short-cuts" the suggested guidance trajectory, such as when a ridge is crossed followed by negative sloping terrain. Further results are found in (Ref. 22).

Near-Field, Pilot-Directed Automated Guidance System

Early efforts at NASA Ames Research Center to reduce pilot workload by automating tasks for NOE flight involved the development of a fully automatic obstacle avoidance system implemented in a real-time workstation based simulation. The technical emphasis of this effort was on the development of guidance and control laws that selected and followed open paths for safe maneuvering based upon the identification of terrain and obstacles from simulated on-board sensor information (Ref. 29). Resulting guidance commands were generated in the form of a 3-dimensional commanded velocity vector. The autopilot-controller, based upon an inversion of the vehicle dynamics, was responsible for computing the cyclic, collective, and rudder control inputs needed to follow the guidance command.

Approach

Following the development of the guidance and control functions for fully automatic flight, research efforts were directed towards the development of an effective means by which a human pilot could interface with the automated systems. The goal was to develop an interface that took advantage of the workload reduction potential of fully automatic guidance and control without compromising pilot confidence and mission flexibility. Qualitative results from previous simulation studies of automated NOE obstacle avoidance systems identified the pilot-interface as being the most crucial factor influencing pilot acceptability (Ref. 30). In particular, studies suggested that poor pilot acceptability would result from any waypoint following, fully automatic NOE system that required pilots to perform merely as system monitors.

Research aimed at identifying effective pilot interface solutions resulted in the selection of a concept referred to as Pilot-Directed Guidance (PDG). The PDG concept, shown schematically in Fig. 9, is based upon a translational velocity-command control system that provides continuous obstacle avoidance protection while depending upon the pilot for overall course guidance (Ref. 31). With this interface, a pilot can concentrate upon primary course guidance and secondary cockpit tasks by delegating obstacle detection and avoidance tasks to the PDG system. The PDG system assists pilots flying NOE by providing: (1) automated obstacle detection and

avoidance, (2) terrain-following altitude control, and (3) airspeed control. PDG relies upon real-time forward-looking sensor information to provide the system with knowledge of obstacles and terrain in the vicinity of the rotorcraft. In the event that the PDG system determines that an obstacle or terrain collision will take place within the PDG look-ahead time window, the necessary avoidance control activity is provided automatically for the pilot. The PDG guidance logic is designed to favor lateral maneuvers over vertical maneuvers in order to provide greater concealment of the vehicle under hostile conditions. Vertical maneuvers are executed by the system in the event that all lateral maneuvering options have been exhausted.

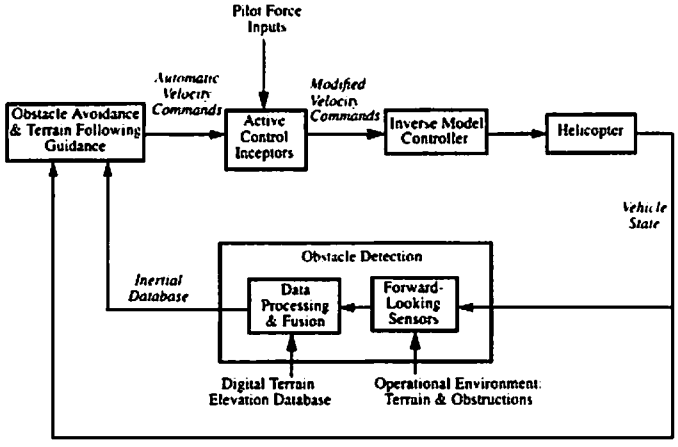

Fig. 9. Near-field, pilot-directed automated guidance system diagram.

Implementation

To improve situational awareness and PDG system monitoring, a Helmet-Mounted Display (HMD) is provided for the pilot. Along with rotorcraft and system state information, the HMD displays inertially referenced course-following symbology that resembles a path-way on the ground described by a series of symbols resembling croquet wickets, as shown in Fig. 10. This course symbology is similar to the pathway in the sky symbology used in the mid-field, low-altitude manual guidance system of the previous section except that the troughs are inverted and anchored to the ground. This provides a more meaningful visual reference to the pilot at very low NOE altitudes. The height of the wickets are set to the PDG commanded radar altitude to provide additional altitude tracking information to the pilot. A ground-based symbol representing the predicted position of the vehicle at the end of the PDG look-ahead time window is also displayed on the HMD. This symbol, referred to as the PDG reference point, resembles an inverted triangle that has its vertex in contact with the terrain surface and its height equal to the PDG commanded radar altitude (Ref. 31). Additional symbology provided, but not shown on Fig. 10, includes a horizon line, boresight indicator, heading indicator, and pitch reference. Automatic obstacle-avoidance control activity is executed whenever a direct line-of-sight to the PDG reference point is obstructed.

To provide a pilot cueing mechanism for automatic control, the cyclic and collective controls are back-driven in the cockpit. The pilot is able to override the PDG system at any time by providing sufficient force input to the control inceptors. The final control inceptor positions, governed by the pilot, are interpreted as the velocity command inputs that are sent to the high bandwidth autopilot controller.

The PDG controller is based upon a non-linear, feedback linearization technique that facilitates its use over the entire flight envelope of the vehicle. The feedback linearization technique is used to transform the input-output map of the original nonlinear system into a linear time-invariant form (Ref. 32). The transformed system is then easily controlled using any well-known linear control design technique. Further simplification of the design process can be realized by dividing the rotorcraft dynamics into multiple time scales of reduced order using the singular perturbation method. The advantage of using this method is that the resulting controllers will also be of reduced order. A baseline nonlinear inverse autopilot design incorporating feedback linearization and time-scale separation was designed and synthesized for a comprehensive flight test validation engineering model of the UH-60A Black Hawk helicopter for the PDG application. The system uses a stored-trim-map approach to approximate the inverse force and moment model of the rotorcraft used during feedback linearization. A simple time-invariant PD-type control law design is used throughout the operational flight envelope.

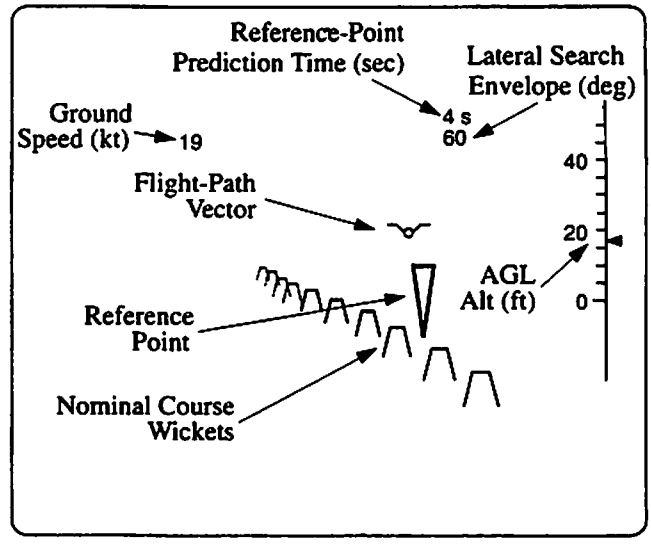

Fig. 10. Near-field, pilot-directed automated guidance system pilot symbology.

Piloted Simulation Results

The control laws of Fig. 9 along with the guidance in display Fig. 10 were evaluated through piloted simulation in the NASA Ames six degree-of-freedom Vertical Motion Simulator (VMS). The Honeywell IHADSS was used as the HMD. Results demonstrated the capability of the PDG automated system to significantly improve flight path performance and reduce pilot workload for NOE missions requiring obstacle avoidance. Flights were conducted both with and without PDG automation for direct comparison of flight path performance and pilot workload. Fig. 11 shows an out-the-window view of the NASA Ames VMS during simulation of the pilot-directed automated guidance system.

Under low visibility conditions, time exposed above tree level was reduced by 75% with the PDG system compared with that of non-automated flights. Increased obstacle clearances, leading to the prevention of obstacle strikes, were also observed with PDG. Secondary performance benefits, resulting from the PDG automation, were greatly improved airspeed and altitude command following. Most importantly, simulation evaluations have demonstrated the potential of the PDG system to substantially reduce overall pilot workload over a range of speed and visibility conditions (Ref. 33).

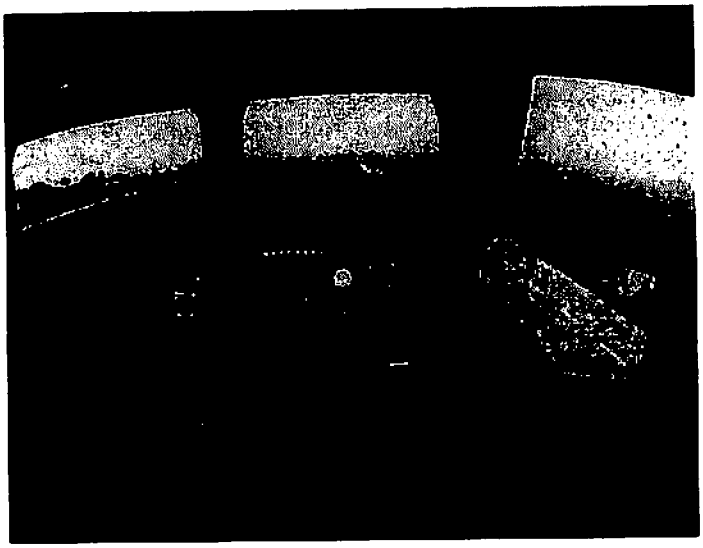

Fig. 11. Pilot's view during simulation of near-field, pilot-directed automated guidance system.

Concluding Remarks

This paper summarizes the status and results of the NASA Automated Nap-of-the-Earth (ANOE) program. A structure involving sensor and database derived guidance, pilot-centered displays, and pilot-automatic control interaction has been employed. Results have been demonstrated through laboratory development, piloted, motion-based simulation, and flight testing in the technology focus areas of passive sensors, active sensors, mid-field manual TF/TA guidance, and near-field pilot-directed NOE automatic guidance.

Algorithms have been developed using calibrated flight test images and a specialized 32-board parallel processor computer that can perform ranging to objects from passive sensors in real-time. Ranging to 300 image objects at 15 Hz through visible-band or infrared cameras have achieved ranging accuracies of 5% given recorded flight test imaging data. Real-time in-flight capability aboard a test helicopter has been demonstrated. Real-time passive ranging to objects has direct application in robotics, airport terminal area operations, and in planetary rovers. Work in passive ranging has supported the external vision component of the NASA high-speed research program, and is applicable to any synthetic-vision system. Calibrated flight test data sets have been distributed to numerous universities and government laboratories.

A scanning, pencil-beam millimeter-wave radar has been developed which can create a local, high-resolution database surrounding an aircraft in real-time for a direct 3-dimensional perspective display. Such an obstacle detection and avoidance capability has immediate value to commercial emergency medical service (EMS) operations, airborne fire-fighting, and oil-rig operations. The millimeter-wave radar system and associated display were flight tested and demonstrated their obstacle detection capability and potential usefulness for collision avoidance.

A mid-field, low-altitude manual guidance system has been developed and extensively flight tested in cooperation with the US Army. When augmented with a laser radar forward-sensor, low-altitude obstacle avoidance capable flights to 75 feet AGL at 80-110 kts were achieved. Guidance trajectories, generated and then modified in real-time by forward-sensor obstacle detections, are presented to the pilot on a helmet-mounted display. This guidance system has direct application to the military and is now being employed in a U.S. Special Operations test program.

A near-field, pilot-directed automated NOE guidance system has been developed and is being refined through piloted, motion-based simulation. The system incorporates back-driven controls and a helmet-mounted display. The system leaves principal and ultimate authority with the pilot while providing an automatic clobber protection capability. Under low visibility conditions, time exposed above tree level was reduced by 75% with this system compared with that of non-automated flights. Increased obstacle clearances, producing no obstacle strikes, were also observed with the pilot-directed guidance system. Simulation evaluations have demonstrated the potential of this pilot-directed automated NOE guidance system to substantially reduce overall pilot workload over a range of speed and visibility conditions.

Future work will focus on the optimal merging of passive sensor and active sensor derived obstacle rangings in creating a local, high-resolution terrain and obstacle database. Work on pilot interaction with automated guidance through pilot-centered displays will continue. Eventual flight demonstration of an integrated automated NOE flight guidance system is conceivable within the coming years.

References

[1]Cheng, V.H.L., and Sridhar, B., "Technologies for Automated Nap-of-the-Earth Flight," *Journal of the American Helicopter Society*, Vol.38, (2), Apr 1993.

[2]Cheng, V.H.L., and Sridhar, B., "Considerations for Automated Nap-of-the-Earth Flight," *Journal of the American Helicopter Society*, Vol. 36, (2), Apr 1991.

[3]Deutsch, O.L., Desai, M., and McGee, L.A., "Far-field Mission Planning for Nap-of-the-Earth Flight," *Proceedings of the AHS national Specialists Meeting on Flight Control and Avionics*, Cherry Hill, N.J., Oct. 1987.

[4]Pekelsma, N.J., "Optimal Guidance with Obstacle Avoidance for Nap-of-the-Earth Flight," NASA TM 177515, Dec. 1988.

[5]Babiak, N., "The Defense Mapping Agency and Tomorrow's Advanced Aerospace Warfare Systems," *Proceedings of the IEEE National Aerospace and Electronics Conference*, Inst. of Electrical and Electronics Engineers, New York, 1990, pp. 260-264.

[6]Denton, R.V., Pekelsma, N.J., Hagen, M., and McGee, L.A., "Guidance Automation for Nap-of-the-Earth Flight," *Proceedings of the 7th Annual Digital Avionics Systems Conference*, Fort Worth, TX, Oct 1986, pp.261-266.

[7]Sridhar, and Phatak, A., "Simulation and Analysis of Image-Based Navigation system for Rotorcraft Low-Altitude Flight," *Proceedings of the American Helicopter Society Specialists' Meeting on Automation Applications of Rotorcraft*, Atlanta, GA, April 1988; IEEE Transactions on Systems, Man and Cybernetics, vol. 22, (2), pp. 96-101, Mar/Apr 1992.

[8]Sridhar, B., Suorsa, R., and Hussien, B., "Passive Range Estimation for Rotorcraft Low-altitude Flight," NASA TM, October 1990.

[9]Suorsa, R. and Sridhar, B., "Validation of Vision Based Obstacle Detection Algorithms for Low Altitude Flight," *Proceedings of the SPIE International Symposium on Advances in Intelligent Systems*, Boston, MA, Nov 1990.

[10]Sridhar, B, Suorsa, R., and Smith, P., "Vision-based Techniques for Low Altitude Flight," *International Symposium on Intelligent Robotics*, Bangalore, India, Jan 1991.

[11]Smith, P.N., Sridhar, B., and Hussien, B., "Vision-Based Range Estimation Using Helicopter Flight Data," *Proceedings of the 1992 IEEE Computer Society Conference on Computer Vision and Pattern Recognition*, Champaign, Illinois, Jun 15-18, 1992; NASA TM 103930, Jun 1992.

[12]Sridhar, B. and Suorsa, R., "Integration of Motion and Stereo Sensors in Passive Ranging Systems," *IEEE Transactions on Aerospace and Electronic Systems*, vol. 27, (4), pp. 741-746, July 1991.

[13]Sridhar, B., Smith, P.N., Suorsa, R.E., and Hussien, B., "Multirate

and Event Driven Kalman Filters for Helicopter Passive Ranging," *Proceedings of the 1st IEEE Conference on Control Applications*, Dayton, Ohio, Sep 1992.

[14]Jacobsen, R.A., Rediess, N.A., Hindson, W.A., Aiken, E.W., and Bivens, C.C., "Current and Planned Capabilities of the NASA/Army Rotorcraft Systems Concepts Airborne Laboratory (RASCAL)," *Proceedings of the American Helicopter Society 51st Annual Forum*, Ft. Worth, TX, May, 1995.

[15]Smith, P.N, Sridhar, B., and Suorsa, R.E., "Multiple-Camera/Motion Stereoscopy for Range Estimation in Helicopter Flight," *Proceedings of the 1993 American Control Conference*, San Francisco, California, Jun 2-4, 1993.

[16]Fong, T.W., and Suorsa, R.E., "Real-time Optical Flow Range Estimation on the iWarp," *Proceedings of the SPIE International Symposium on Intelligent Information Systems*, Orlando, Florida, Apr 1993.

[17]Suorsa, R.E., Sridhar, B., and Fong, T.W., "Real-Time Computational Needs of a Multisensor Feature-Based Range-Estimation Method," *Proceedings of the SPIE International Symposium on Optical Engineering and Photonics in Aerospace Science and Sensing: Sensor Fusion and Aerospace Applications*, Orlando, Florida, Apr 1993.

[18]Karmarkar, J.S., and Sridhar, B., and Lakshmanan, M., "Cost-effective Implementation of Passive Ranging Algorithms on General Purpose Parallel Architectures," *Proceedings of the SPIE International Symposium on Optical Engineering and Photonics in Aerospace Science and Sensing: Sensor Fusion and Aerospace Applications*, Orlando, Florida, Apr 1993.

[19]Suorsa, R.E., and Sridhar, B., "A Parallel Implementation of a Multisensor Feature-Based Range-Estimation Method," *Proceedings of the 1993 IEEE Computer Society Conference on Computer Vision and Pattern Recognition*, New York, New York, Jun 1993.

[20]Sridhar, B., and Suorsa, R.E., "Computer Architectures for a Real-time Passive Ranging Algorithm," *Proceedings of the IEEE/AIAA Digital Avionics Systems Conference*, Ft. Worth, 1993.

[21]Becker, Robert C., and Almsted, L.D., "Flight Test Evaluation of a 35 GHz Forward Looking Altimeter for Terrain Avoidance," *Proceedings of the IEEE/AIAA Digital Avionics Systems Conference*, Phoenix, 1994.

[22]Zelenka, R.E., Clark, R.F., Zirkler, A., Saari, R., and Branigan, R.G., "Development and Flight Test of Terrain-Referenced Guidance with Ladar Forward Sensor," *AIAA Journal of Guidance, Control, and Dynamics*, Vol. 19, No. 4, 1996, pp. 823-828.

[23]Zelenka, R.E., and Almsted, L.D., "Flight Test of a 35 GHz Radar Forward Sensor for Collision Avoidance," *Proceedings of the SAE/AIAA First World Aviation Congress*, Los Angeles, Oct 22-24, 1996.

[24]Swenson, H.N., Zelenka, R.E., Hardy, G., and Dearing, M., "Simulation Evaluation of a Low-Altitude Helicopter Flight Guidance System," *Proceedings of the 10th IEEE/AIAA Digital Avionics Systems Conference* (Los Angeles, CA), 1991.

[25]Swenson, H.N., Jones, R.D., and Clark, R.F.; "Flight Evaluation of a Computer Aided Low-Altitude Helicopter Flight Guidance System," NATO AGARD CP-520 Flight Mechanics and Guidance and Control Panel Symposium, Edinburgh, UK, Oct. 19-22, 1992.

[26]Zelenka, R.E., Yee, Z., and Zirkler, A., "Flight Test of a Radar Altimeter Enhancement for Terrain-Referenced Guidance," *AIAA Journal of Guidance, Control, and Dynamics*, Vol. 18, (4), 1995, pp. 702-708.

[27]Branigan, R., "Design Requirements for an Obstacle Avoidance System (OASYS)," U.S. Army CNVEO Report, Jul 1992.

[28]Holder, S., and Dillon, R., "Army Helicopter Obstacle Avoidance System (OASYS): Performance Modeling and Preliminary Performance Data," *Proceedings, IRIS Specialty Group on Active Systems*, Oct 1992.

[29]Cheng, V.H.L. "Concept Development of Automatic Guidance & Control for Helicopter Obstacle Avoidance," *Proceedings of the IEEE International Conference on Robotics and Automation*, Nice, France, pp. 252-260, May 1-12, 1992.

[30]Coppenbarger, R.A., and Cheng, V.H.L., "Concepts for Pilot Interaction with an Automated NOE Obstacle Avoidance System," *Proceedings of the AIAA Guidance, Navigation, and Control Conference*, Hilton Head Island, SC, Aug 10-12, 1992.

[31]Coppenbarger, R.A., "Helmet-Mounted Display Symbology for Automated Nap-of-the-Earth Rotorcraft Flight," *Proceedings of the SPIE Conference on Helmet-and Head-Mounted Display & Symbology Requirements*, Orlando, FL, Apr 5-7, 1994.

[32]Njaka, C.E., Menon, P.K., and Cheng, V.H.L., "Towards an Advanced Nonlinear Rotorcraft Flight Control System Design," *Proceedings of the IEEE/AIAA Digital Avionics Systems Conference*, Phoenix, 1994, pp. 190-197.

[33]Coppenbarger, R.A., "A Sensor-Based Automated Obstacle Avoidance System for Nap-of-the-Earth Rotorcraft Missions," *Proceedings of the SPIE Conference on Helmet-and Head-Mounted Display & Symbology Requirements*, Orlando, FL, Apr 10-14, 1995.